DOI: 10.48011/sbse.v1i1.2316

Sinusoidal PWM techniques comparison for the Quasi-Y-Source Inverter

Rafael dos Santos [*] **Flávio A. S. Gonçalves** [*]

[*] *Institute of Science and Techonology of Sorocaba, UNESP, SP, Brazil (e-mails: rafael.santos1994@unesp.br, flavio.as.goncalves@unesp.br).*

Abstract: Impedance networks inverters (INI) have emerged as an alternative to improve traditional inverters, allowing their operation as a buck-boost type converter, through the utilization of the "shoot-through" conduction state, where switches of one or more inverter legs are gated on simultaneously. Recently introduced, the Quasi-Y-Source inverter (QYSI) is a magnetic coupled INI that has particular performance advantages, specially for renewable sources and distributed generation. To control the QYSI there is several techniques based on Sinusoidal Pulse Width Modulation (SPWM), that are modified to allow the shoot-through state. This work aims to present, through computational simulations, a comparative analysis of three SPWM techniques applied in three-phase QYSI, considering a fixed boost factor and a three-phase/three-wire RL load connected to the inverter output. The following modulation techniques were compared: Simple Boost Control (SBC), Maximum Boost Control with third harmonic injection (MBC_{3h}) and Maximum Constant Boost Control with third harmonic injection (MCBC_{3h}). Simulation results show operation characteristics of the QYSI for the different modulation techniques. A Fourier analysis was performed in order to evaluate harmonic distortion and harmonic spectrum for both inverter output voltage and current, and a comparative analysis was performed showing several relationships among voltage gain, switch voltage stress, shoot-through duty ratio and modulation index for the different SPWM techniques. Simulation results shows the advantages and disadvantages of each SPWM technique applied to QYSI and the impact of the coupled inductor on inverter performance, helping to establish proper criteria for choosing among SPWM techniques for different power systems applications.

Keywords: Quasi-Y-Source, Inverter, Distributed Generation, SPWM, Impedance Networks.

1. INTRODUCTION

The development of INI was originally done to overcome the limitations associated with conventional inverters based on voltage source (VSI) or current source (CSI), due to: (a) The activation of switches located on same inverter leg, by EMI or undesired control actions; (b) The buck type characteristic of these converters, which limits the magnitude of the inverter AC output voltage.

The Z-Source inverter, proposed by Peng (1999), was the first INI, and its mode of operation remains the same for most of the topologies developed afterwards. The Z-Source inverter has two states of operation: (a) Active state; (b) Shoot-through state. In the active state, the power source is connected directly to the load, and the inverter operates in the traditional manner. In the shoot-through state, the upper and lower switches located at one or more inverter legs, are activated simultaneously (shoot-through conduction). Unlike traditional VSI and CSI converters, this scenario is now possible due to the specific topology of impedance networks, which disconnect the power supply from the rest of the circuit when shoot-through conduction occurs, and promotes a particular energy management on the impedance network energy storage devices, which makes possible the buck-boost operation. There are several topologies for impedance network converters present in the literature, for different applications, and as observed by Shults et al. (2015), these converters are based on different combinations of energy storage elements, such as inductors and capacitors, and may contain diodes and other power switches which make possible a bidirectional energy flow and promotes an improvement in performance and efficiency. A generic representation of an impedance network converter can be seen in Figure 1.

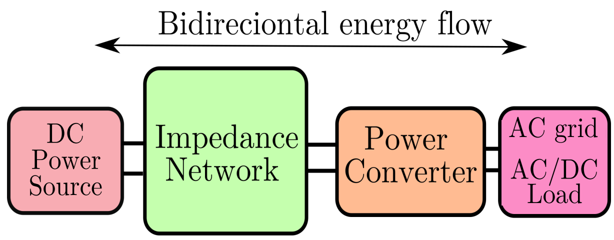

Figure 1. Scheme of an impedance network converter.

The QYSI, proposed by Siwakoti et al. (2015), is a magnetic coupled based INI that promotes high voltage gain, less voltage stress on inverter switches, and continuous conduction at the input stage, with the utilization of cheaper components, which is required by many renewable sources and distributed power generation applications. Ac-

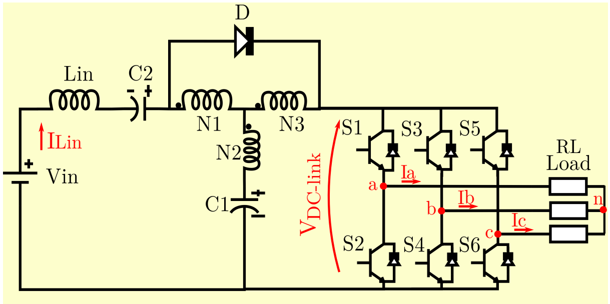

Figure 2. QYSI circuit schematic.

cording to Siwakoti et al. (2014) the modulation techniques to control three-phase INI can be broadly categorized as SPWM and space-vector PWM (SVPWM). In this sense, given the great number of SVPWM techniques and their different arrangements, as compared by Liu et al. (2013), this paper is going to focus on the SPWM techniques.

Therefore, given the different aspects of the SPWM techniques, and the potential of QYSI, although there are some works that have compared these different modulation techniques for impedance source converters such as the studies conducted by Loh et al. (2006), Rostami and Khaburi (2009), Ellabban et al. (2009), Husodo et al. (2010), Suganthi and Rajaram (2015) and Abdelhakim et al. (2018), there is still no comparative analysis of these methods applied for the QYSI.

Hence, this work aims to present, through computational simulations, a comparative analysis among the SBC, MBC_{3h} and MCBC_{3h} modulation techniques, introduced by Peng (1999), Peng et al. (2005) and Shen et al. (2004) respectively; applied in three-phase QYSI. The simulated operation must provide constant power to feed a three-phase/three-wire wye connected RL load at inverter output, as shown in Figure 2. An analysis is then made, for each SPWM technique, based on: (a) A comparison, of input current $I_{Lin}(t)$, DC link voltage $V_{DC-link}(t)$ and load phase current $(I_{a,b,c}(t))$ and voltage $(V_{an,bn,cn}(t))$; (b) A Fourier transform analysis in order to evaluate total harmonic distortion (THD) and harmonic spectrum, for both inverter output phase voltage and current; (c) The establishment of relationships among voltage gain, switch voltage stress, shoot-through duty ratio and modulation index.

This paper is organized as follows: section 2 shows the basic mathematical description of the QYSI, in section 3 the SPWM techniques are presented, in section 4 the basic concept of third harmonic injection is presented, and simulation results are shown in section 5 with conclusions made on section 6.

2. QUASI-Y-SOURCE INVERTER

The QYSI consists of a three-phase/three-wire inverter bridge configuration, connected to an impedance network formed by a coupled inductor with three windings N_1, N_2, N_3; two capacitors C_1 and C_2, an inductor L_{in} and the diode D. In the QYSI there are two stages of operation, defined as: (a) Shoot-through state; (b) Active state; as shown on Figures 3-a) and b), respectively. In this paper, the shoot-through conduction mode is defined

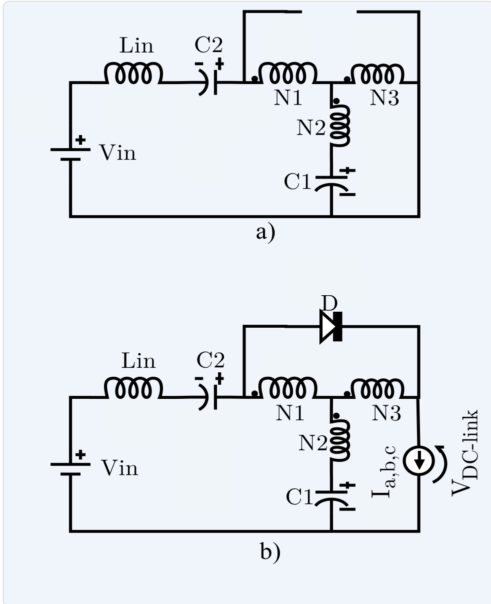

Figure 3. States of QYSI: a) Shoot-through, b) Active.

Table 1. Correlation among δ, D_{st} and different configurations of N_1:N_2:N_3.

δ	D_{st-max}	**N1:N2:N3**
2	0.50	(1:3:1), (2:4:1), (3:5:1)
3	0.33	(1:2:1), (3:3:1), (2:4:2)
4	0.25	(2:2:1), (1:3:2), (5:3:1)
5	0.20	(3:2:1), (2:3:2), (1:4:3)
6	0.17	(4:2:1), (3:3:2), (2:4:3)

as all inverter bridge switches $(S_1 - S_6)$ turned on simultaneously.

Equation (1) determines the peak value of the QYSI DC link voltage, where V_{in} is the input voltage, $\delta = \frac{N_1+N_2}{N_2-N_3}$ is the winding factor for different N_1, N_2, N_3 turns ratio, and the shoot-through duty ratio D_{st} is defined by (2), being T_s and T the shoot-through and switching periods, respectively. For the output phase voltage, the peak amplitude of the fundamental-frequency component is expressed by (3), where B is the boost factor provided by the impedance network, and M is the linear modulation index. For the QYSI, $B = \frac{1}{1-\delta D_{st}}$, and for different definitions of δ, a maximum value of D_{st} is allowed, defined by $\frac{1}{\delta}$, as shown in Table 1. The factor G is the inverter voltage gain, defined as $G = MB$. The voltage stress V_s imposed on inverter switches is defined by (4).

$$\hat{V_{DClink}} = \frac{1}{1-\delta D_{st}} V_{in} \tag{1}$$

$$D_{st} = \frac{T_s}{T} \tag{2}$$

$$\hat{V_{1ph}} = MB\frac{V_{in}}{2} = G\frac{V_{in}}{2} \tag{3}$$

$$V_s = BV_{in} \tag{4}$$

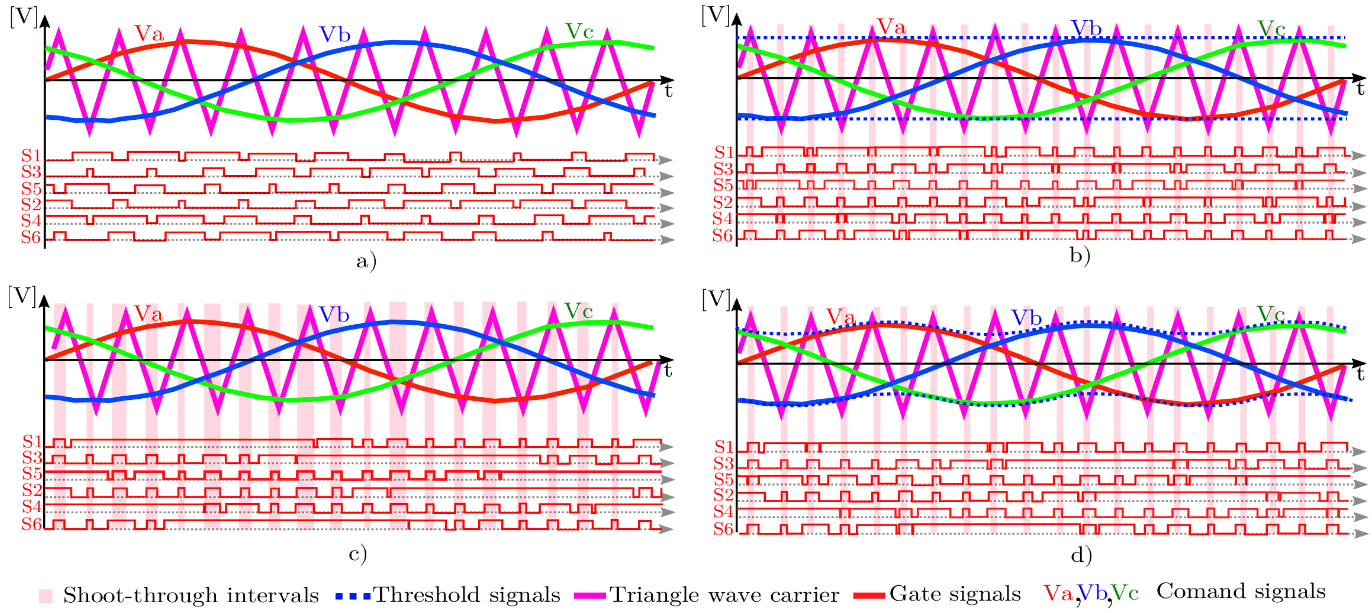

Figure 4. Examples of different SPWM techniques: a)Traditional technique, b)SBC, c)MBC, d)MCBC.

3. MODIFIED SPWM TECHNIQUES

In the traditional SPWM technique, as depicted in Figure 4-a), the inverter switches are complementarily controlled and the activation of switches located on the same inverter leg are forbidden. The switches activation are based on the comparison between the triangular wave carrier $V_{tri}(t)$, and the sinusoidal command signals $V_{a,b,c}(t)$, accordingly with (5) and (6), where S_+ and S_- are, respectively, the switches located on the upper and lower position of the same inverter leg.

$$V_{a,b,c}(t) \geq V_{tri}(t) \rightarrow S_+ : On,\, S_- : Off \qquad (5)$$
$$V_{a,b,c}(t) < V_{tri}(t) \rightarrow S_+ : Off,\, S_- : On \qquad (6)$$

In order to control the QYSI, it is necessary to modify the traditional SPWM technique, in order to include the shoot-through conduction mode. Therefore, the SBC, MBC and MCBC techniques, shown respectively on Figures 4-b), c), d); are common modified SPWM strategies. The differences among these techniques relies on how shoot-through conduction is achieved, which is briefly described bellow.

3.1 Simple Boost Control

The SBC technique, as shown in Figure 4-b), is based on the use of two constant and symmetrical threshold control signals, whose values are equal to $\pm M$. When $V_{tri}(t)$ has a magnitude greater than the positive threshold, or lower than the negative threshold, the inverter switches are set in shoot-through conduction mode. Otherwise, the inverter operates accordingly with the traditional SPWM.

3.2 Maximum Boost Control

The MBC technique, as shown in Figure 4-c), is based on the SPWM null conduction states, where no voltage is supplied to the load, and do not make use of threshold control signals. Therefore, shoot-through conduction occurs when $V_{tri}(t)$ is greater than the maximum, or lower than the minimum values of all three reference sinusoidal signals $V_{a,b,c}(t)$.

3.3 Maximum Constant Boost Control

The MCBC technique, as shown in Figure 4-d), working principle is similar to the SBC technique, but now the threshold control signals are sinusoidal, and defined by (7), when $0 \leq \theta \leq \frac{\pi}{3}\, rad.$ and (8) when $\frac{\pi}{3} \leq \theta \leq \frac{2\pi}{3} rad.$, where $\theta = 2\pi f_s t\, rad.$, and f_s is the load frequency.

$$V_{p1} = M(\sqrt{3} + sin(\theta - \frac{2\pi}{3})),\; V_{n1} = Msin(\theta - \frac{2\pi}{3}) \quad (7)$$
$$V_{p2} = Msin(\theta),\; V_{n2} = M(sin(\theta) - \sqrt{3}) \qquad (8)$$

4. THIRD HARMONIC INJECTION

The use of third harmonic injection, as proposed by Grant and Houldsworth (1984), in all modified SPWM techniques, can increase G while maintaining the same B, because the maximum range of M is increased from 1 to $\frac{2}{3}\sqrt{3}$. Moreover, third harmonic injection can simplify the implementation of MCBC technique, as observed by Shen et al. (2004), by turning the threshold control signals into straight lines, defined by $\pm\frac{\sqrt{3}}{2}M$. Using third harmonic injection with SBC and MCBC technique results in the same modulation scheme, therefore only the MCBC_{3h} technique will be explored in this paper.

The technique consists of inserting three additional sine waves into $V_{a,b,c}(t)$ reference signals, defined by (9). In this paper, the subscript "3h" indicates the injection of third harmonic.

$$V_{3rd}(t) = \frac{1}{6}Msin(3\omega t) \qquad (9)$$

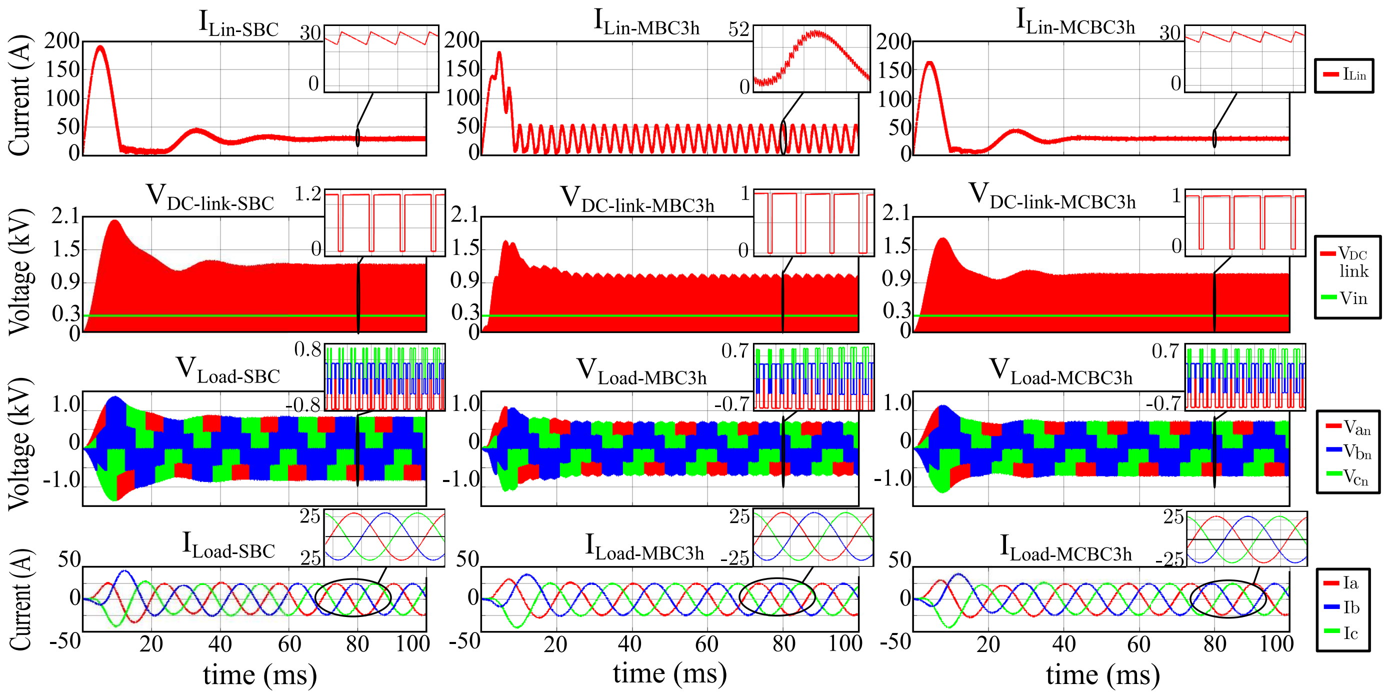

Figure 5. $I_{Lin}(t)$, $V_{DC-link}(t)$, $V_{an,bn,cn}(t)$ and $I_{a,b,c}(t)$ for SBC, MBC$_{3h}$ and MCBC$_{3h}$.

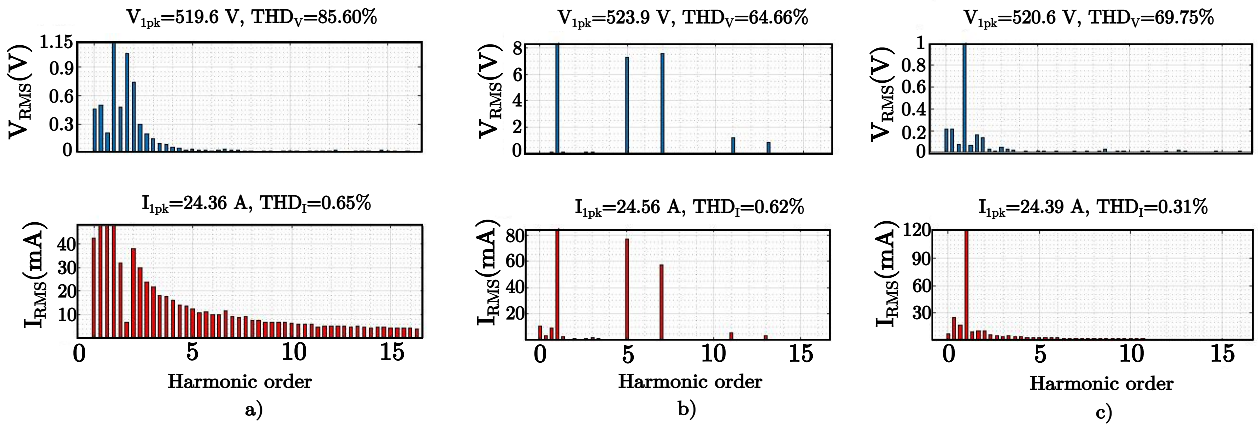

Figure 6. FFT analysis for phase voltage (blue) and phase current (red) for: a) SBC, b)MBC$_{3h}$ and c) MCBC$_{3h}$.

5. SIMULATION

5.1 Simulation parameters

The simulation was conducted using the SBC, MBC$_{3h}$ and MCBC$_{3h}$ SPWM methods, using the ode23t trapezoidal solver and variable step time, with minimum step size of 50 ns. The following values were used for the three-phase/three-wire QYSI: $V_{in} = 300\ V$, $L_{in} = 5\ mH$, $\delta = 5$, $C_{1,2} = 120\ \mu F$, N_1:N_2:N_3 = 3:2:1. The inverter three-phase load parameters are: $P_o = 9\,kW$, $L = 50\ mH$, $R = 10\ \Omega$ with $f_s = 60\ Hz$. For all methods the triangle wave frequency was set to $f_{tri} = 10\ kHz$. The modulations index M for SBC, MBC$_{3h}$ and MCBC$_{3h}$ were set to 0.8485, 1.0392, 0.9890 respectively, in order to have $\hat{V_{1ph}} = 525\ V$ for all modulation techniques, obtained by the formulae available in Table 2. The FFT analysis was performed within 50 ms-217 ms time window , with ten 60 Hz sine wave cycles.

Table 2. Indexes definitions for SBC, MBC$_{3h}$ and MCBC$_{3h}$ techniques.

Index	**SBC**	**MBC$_{3h}$**	**MCBC$_{3h}$**
D_{st}	$1-M$	$\frac{2\pi-3\sqrt{3}M}{2\pi}$	$1-\frac{\sqrt{3}M}{2}$
B	$\frac{1}{1+\delta(M-1)}$	$\frac{1}{1+\delta(\frac{3\sqrt{3}M}{2\pi}-1)}$	$\frac{1}{1+\delta(\frac{\sqrt{3}M}{2}-1)}$
G	$\frac{M}{1+\delta(M-1)}$	$\frac{M}{1+\delta(\frac{3\sqrt{3}M}{2\pi}-1)}$	$\frac{M}{1+\delta(\frac{\sqrt{3}M}{2}-1)}$
V_s	$\frac{V_{in}}{1+\delta(M-1)}$	$\frac{V_{in}}{1+\delta(\frac{3\sqrt{3}M}{2\pi}-1)}$	$\frac{V_{in}}{1+\delta(\frac{\sqrt{3}M}{2}-1)}$
$M:$	$(\frac{\delta-1}{\delta},1]$	$(\frac{2\pi(\delta-1)}{3\sqrt{3}\delta},\frac{2\sqrt{3}}{3}]$	$(\frac{2(\delta-1)}{\sqrt{3}\delta},\frac{2\sqrt{3}}{3}]$

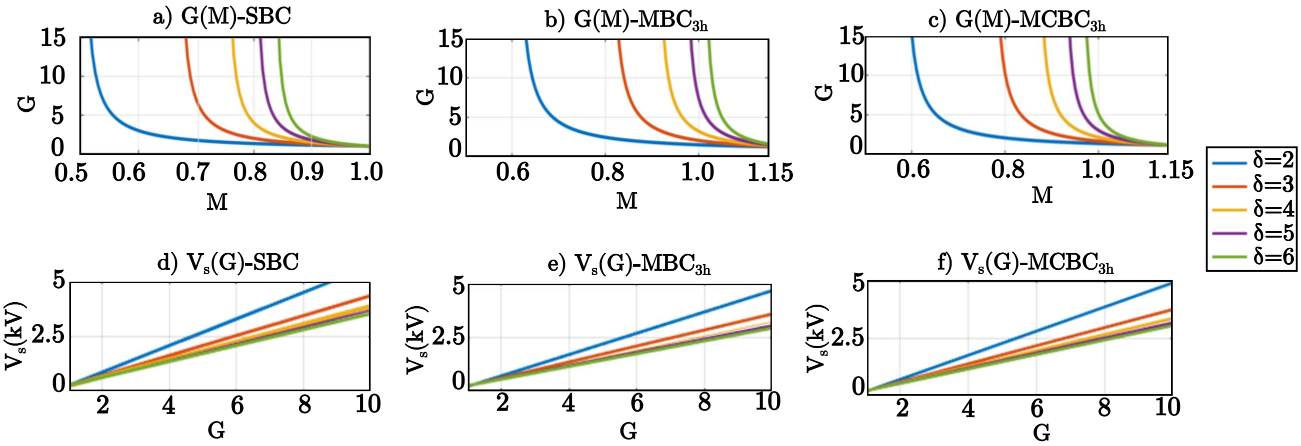

Figure 7. Functions $G(M)$ and $V_s(G)$ for SBC, MBC$_{3h}$ e MCBC$_{3h}$ techniques, for different δ values.

5.2 Comparative analysis

This subsection presents the comparative analysis among SPWM techniques for the following criteria: Input current $I_{Lin}(t)$, DC link voltage $V_{DC-link}(t)$, modulation index M, switch voltage stress V_s, shoot-through duty ratio D_{st} and the functions $G(M)$ and $V_s(G)$. Simulations results are depicted on Figures (5) and (6). A summary of this analysis is presented in Table 3, where the SPWM techniques were rated from $\star$ to $\star\star\star$ according to its performance on different evaluation criteria.

Input current ($I_{Lin}(t)$): Comparing the techniques with respect to the input current $I_{Lin}(t)$, the MBC$_{3h}$ method presents the greatest current ripple, due to the oscillation of D_{st} provided by this method, as can be seen in Figure 4-c), whereas SBC and MCBC$_{3h}$ had similar behavior. SBC promotes the biggest peak current value during the transient period, followed by MBC$_{3h}$ and MCBC$_{3h}$. The absence of equivalent series resistances caused current and DC link voltage overshoot, observed at transient regime for all techniques.

DC link voltage ($V_{DC-link}(t)$): Comparing the techniques with respect to DC link voltage $V_{DC-link}(t)$, all methods reached similar results, however with small differences due to D_{st} variation, evident for MBC$_{3h}$ by the same reason given earlier. However, the low frequency voltage oscillation inserted by MBC$_{3h}$ in $V_{DC-link}(t)$, creates higher voltage harmonic components when compared to SBC and MCBC$_{3h}$, despite the fact that the THD component for this technique is smaller than the other two, as can be seen in Figure 6. This happens because, unlike SBC and MCBC3a, the shoot-through conduction occurs at the null states, inserting less harmonic content at the voltage output. By the FFT analysis as shown in Figure 6, it can be seen that the MCBC$_{3h}$ technique had the lowest THD for load current, followed by MBC$_{3h}$ and SBC. Nevertheless, MBC$_{3h}$ reached the permanent regime faster than the other techniques.

Modulation index (M) As shown on Figures 7-a), b) and c), for all modified SPWM techniques, the lower the values of δ, wider will be the range of M. Theoretically, if M is not set at the interval defined in Table 2, G will tend to infinity, may causing the destruction of inverter switches due to high voltage stress.

Switch voltage stress (V_s): As can be observed on Figures 7-d), e) and f), the MBC$_{3h}$ and MCBC$_{3h}$ control techniques does not present significant differences in the magnitudes of V_s, but SBC provides the greatest V_s, for the same M.

Although the MBC$_{3h}$ allows a much greater G than MCBC$_{3h}$ for the same value of M, as can be seen on Figures 7-a), b) and c), the voltage stress related to the operation in shoot-through conduction mode will be greater too, when compared to the use of MCBC$_{3h}$ and SBC, due to high values of B.

It can also be observed that higher values of δ provides lower values of V_s on switches. Therefore, the MBC$_{3h}$ technique could be more interesting for scenarios where a greater value of δ could be implemented with more reliable switches technologies, such as the ones based on SiC or GaN for example. Nevertheless, MCBC$_{3h}$ technique brings an interesting compromise between G and switches reliability.

Shoot-through duty ratio (D_{st}): According to Siwakoti et al. (2014), due to the variable D_{st} promoted by MBC$_{3h}$ technique, there is additional low frequency ripple components for both $V_{DC-link}(t)$ and $I_{Lin}(t)$ in QYSI impedance network, which causes an oversize design of devices, increasing the volume and cost of the converter. This is not the case for SBC and MCBC$_{3h}$.

6. CONCLUSION

This article presented a comparative analysis among three SPWM techniques: SBC, MBC$_{3h}$ and MCBC$_{3h}$, applied for QYSI. It was showed that each SPWM technique has

Table 3. Summary of SPWM comparison.

Category	*Aspects*	*SBC*	MBC_{3h}	$MCBC_{3h}$
Transient regime	I_{Lin-pk}	⋆	⋆⋆	⋆⋆⋆
	$V_{DC-link-pk}$	⋆	⋆⋆	⋆⋆⋆
	Duration	⋆	⋆⋆⋆	⋆⋆
Ripple	$I_{Lin}(t)$	⋆⋆	⋆	⋆⋆⋆
	$V_{DC-link}(t)$	⋆⋆	⋆	⋆⋆⋆
THD	$V_{Load}(t)$	⋆	⋆⋆⋆	⋆⋆
	$I_{Load}(t)$	⋆	⋆⋆	⋆⋆⋆
M	*Range vs.* V_s	⋆	⋆⋆	⋆⋆⋆
QYSI design	*Volume & cost*	⋆⋆	⋆	⋆⋆⋆

its own advantages and disadvantages, depending of the purpose of application. In this sense, SBC technique is preferable because of it ease of implementation, but on the other hand, presents the worst performance in several aspects when compared to MBC_{3h} and MCBC_{3h}. MBC_{3h} is interesting when a fast response and low harmonic content in phase voltage is desired. It also allows the maximum G for different M values. However, an additional volume and cost will be present on the QYSI impedance network design, due to high input current and inverter DC link voltage ripple content. MCBC_{3h} presents several advantages when compared to other techniques, with a fair performance regarding time response and phase voltage harmonic content, with a design implementation that has the same complexity as SBC technique. In this sense, MCBC_{3h} appears as an interesting SPWM technique to be applied in the system consisting of a three-phase/three-wire QYSI feeding a RL load connected in wye.

7. ACKNOLEDGEMENTS

This project was financially supported by #2016/08645-9 and #2018/24331-0 grants, São Paulo Research Foundation (FAPESP).

REFERENCES

Abdelhakim, A., Blaabjerg, F., and Mattavelli, P. (2018). Modulation schemes of the three-phase impedance source inverters—part ii: Comparative assessment. *IEEE Transactions on Industrial Electronics*, 65(8), 6321–6332.

Ellabban, O., Van Mierlo, J., and Lataire, P. (2009). Comparison between different pwm control methods for different z-source inverter topologies. In *2009 13th European Conference on Power Electronics and Applications*, 1–11. IEEE.

Grant, D. and Houldsworth, J. (1984). Pwm ac motor drive employing ultrasonic carrier. In *IEE Conf. PE-VSD*, 234–240.

Husodo, B., Anwari, M., Ayob, S., et al. (2010). Analysis and simulations of z-source inverter control methods. In *2010 Conference Proceedings IPEC*, 699–704. IEEE.

Liu, Y., Ge, B., and Abu-Rub, H. (2013). Theoretical and experimental evaluation of four space-vector modulations applied to quasi-z-source inverters. *IET Power Electronics*, 6(7), 1257–1269.

Loh, P.C., Blaabjerg, F., and Wong, C.P. (2006). Comparative evaluation of pulse-width modulation strategies for z-source neutral-point-clamped inverter. In *2006 37th IEEE Power Electronics Specialists Conference*, 1–7. IEEE.

Peng, F.Z. (1999). Z-source inverters. *Wiley Encyclopedia of Electrical and Electronics Engineering*, 1–11.

Peng, F.Z., Shen, M., and Qian, Z. (2005). Maximum boost control of the z-source inverter. *IEEE Transactions on power electronics*, 20(4), 833–838.

Rostami, H. and Khaburi, D. (2009). Voltage gain comparison of different control methods of the z-source inverter. In *2009 International Conference on Electrical and Electronics Engineering-ELECO 2009*, I–268. IEEE.

Shen, M., Wang, J., Joseph, A., Peng, F.Z., Tolbert, L.M., and Adams, D.J. (2004). Maximum constant boost control of the z-source inverter. In *Conference Record of the 2004 IEEE Industry Applications Conference, 2004. 39th IAS Annual Meeting.*, volume 1. IEEE.

Shults, T.E., Husev, O.O., and Zakis, J.G. (2015). Overview of impedance source networks for voltage source inverters. In *2015 16th International Conference of Young Specialists on Micro/Nanotechnologies and Electron Devices*, 514–520. IEEE.

Siwakoti, Y.P., Blaabjerg, F., and Loh, P.C. (2015). Quasi-y-source inverter. In *2015 Australasian Universities Power Engineering Conference (AUPEC)*, 1–5. IEEE.

Siwakoti, Y.P., Peng, F.Z., Blaabjerg, F., Loh, P.C., and Town, G.E. (2014). Impedance-source networks for electric power conversion part i: A topological review. *IEEE Transactions on power electronics*, 30(2), 699–716.

Suganthi, J. and Rajaram, M. (2015). Effective analysis and comparison of impedance source inverter topologies with different control strategies for power conditioning system. *Renewable and Sustainable Energy Reviews*, 51, 821–829.